International Journal of Mass Spectrometry 297 (2010) 116–123

Contents lists available at ScienceDirect

International Journal of Mass Spectrometry

journal homepage: www.elsevier.com/locate/ijms

Effects of anions on the zwitterion stability of Glu, His and Arg investigated by IRMPD spectroscopy and theory

Jeremy T. O'Brien[a], James S. Prell[a], Giel Berden[b], Jos Oomens[b,c], Evan R. Williams[a,*]

[a] Department of Chemistry, University of California, Berkeley, CA 94720-1460, United States
[b] FOM Institute for Plasma Physics "Rijnhuizen", Edisonbaan 14, 3439 MN, Nieuwegein, The Netherlands
[c] Van't Hoff Institute for Molecular Sciences, University of Amsterdam, Amsterdam, The Netherlands

ARTICLE INFO

Article history:
Received 11 May 2010
Received in revised form 30 June 2010
Accepted 1 July 2010
Available online 18 July 2010

Keywords:
Amino acid
Zwitterion
Infrared multiple photon dissociation spectroscopy
IRMPD
Anion

ABSTRACT

Interactions of halide anions (Cl^-, Br^-, and I^-) with glutamic acid (Glu), histidine (His), and arginine (Arg) and their effects on stabilizing the zwitterionic form of these amino acids were investigated using infrared multiple photon dissociation (IRMPD) spectroscopy between 850 and 1900 cm^{-1} and hybrid density functional theory. The IRMPD spectra of Glu·X^- and His·X^- each have a diagnostic carbonyl stretching band at ~1750 cm^{-1} from a carboxylic acid group, indicating that the nonzwitterionic form of these amino acids is most stable. In contrast, a broad band at ~1625 cm^{-1} for Arg·X^-, consisting of the antisymmetric stretch of a carboxylate group and hydrogen bonded NH bends, clearly shows that Arg is zwitterionic in these complexes. There are many similarities between these spectra and those of cationized amino acids, which aid in spectral interpretation. Cl^- and Cs^+ are of comparable size, and attachment of either ion to these amino acids has little effect on the frequencies of these diagnostic carbonyl stretches. The coordination of cations to these amino acids is different from that of anions, resulting in a favorable alignment of the dipole moment of the carbonyl group with the electric field of ions of either polarity, which causes a redshift in this band, i.e., a Stark effect. There is a slight redshift (~10 cm^{-1}) in the carbonyl stretch band at ~1750 cm^{-1} for Glu·X^- and His·X^- with decreasing anion size, consistent with both a Stark effect and with greater carboxylate character for the carboxylic acid group in complexes with the less acidic halide ions. The anion size has little effect on the structures and relative zwitterion stabilities for most of these complexes, which can be attributed to the large size of the halide anions investigated compared to that of the alkali metal cations where size effects are more pronounced. The spectra calculated for the lowest energy structures are generally consistent with the experimental spectra, although no single structure accounts for the many distinct bands in the IRMPD spectra of His·X^-.

1. Introduction

Ions are important in many aspects of biology, including protein structure and complex assembly [1–3], neuron signaling [4,5], immune response [6], and pH regulation [7,8]. Ion–protein interactions occur during ion transport through cell membranes and play a critical role in regulating ion concentrations in the body. For example, cystic fibrosis is a life-threatening condition caused by defects in a protein that transports chloride ions across cell membranes [9]. Ions also affect protein solubility. The effects of ions on protein stability were first measured in the 1880s, and the ordering of ions based on their ability to precipitate proteins is known as the Hofmeister series [10,11]. The effects of anions on protein solubility in aqueous solutions are generally stronger than those of cations, although solvent effects may play a significant role in this difference. The precise chemical origins of the Hofmeister series are still debated today [12–16]. Understanding the interactions of ions and proteins in solution is a complex problem that is complicated by effects of solvation, counter-ions, and protein structure.

Infrared multiple photon dissociation (IRMPD) spectroscopy has been used to probe the structures of ionized complexes in the gas phase and is potentially a powerful tool for understanding ion–protein interactions. An important advantage of this technique is the ability to investigate the structures of biomolecules in isolation, where complicating structural effects of solvent and counter-ions are absent. The interactions of metal cations with amino acids, the building blocks of proteins, have been extensively investigated using IRMPD spectroscopy [17–38]. IRMPD spectra have been reported for amino acids complexed with both mono- [19–38] and divalent cations [17,18,28–31]. In isolation,

* Corresponding author at: Department of Chemistry, University of California, 410 Latimer Hall #1460, Berkeley, CA 94720-1460, United States.
Tel.: +1 510 643 7161; fax: +1 510 642 7714.
E-mail address: williams@cchem.berkeley.edu (E.R. Williams).

1387-3806/$ – see front matter © 2010 Elsevier B.V. All rights reserved.
doi:10.1016/j.ijms.2010.07.003

all naturally occurring amino acids are nonzwitterionic, but the zwitterionic form can be preferentially stabilized by the addition of a metal cation. Effects of metal ion size [19–25,28–30,32–34], charge state [17,18,28–31,39], and amino acid basicity/acidity [19–21,30,40–44] on the relative stability of zwitterionic structures have been extensively studied. These studies indicate that for some amino acids, zwitterionic structures are preferentially stabilized with increasing metal ion size [23–25,28,32] and higher charge state [17,18,28,30] and with increasing amino acid basicity [19–21,30,40–44], although other factors can compete to stabilize nonzwitterionic forms [20,21,43]. Trp [18], His [28], Arg, Gln, Pro, Ser, Val [17], and Glu [30] complexed with Ba^{2+} are zwitterionic, but nonzwitterionic structures have been reported for some doubly charged complexes, including His·Ca^{2+} [28] and Asn·Ba^{2+} [29].

In contrast to results for cations, much less is known about anion interactions with amino acids and to what extent they stabilize their zwitterionic forms. Attachment of an excess electron can stabilize the zwitterionic form of Arg [45,46]. Complexes of the dianion of oxalic or malonic acid with the zwitterionic form of glycine were investigated computationally and were each found to be metastable with relatively low barriers to dissociation [47]. IRMPD spectra of deprotonated amino acids (Asp, Cys, Glu, Phe, Ser, Trp, and Tyr) were recently reported [48]. These spectra are dominated by bands corresponding to carboxylate stretching modes, and for Glu and Asp, the IRMPD spectra have very broad, poorly resolved features which are attributed to the sharing of a proton between the side chain and C-terminal carboxylate groups.

Here, we report the first IRMPD spectra of anionized amino acids, Glu·X^-, His·X^- and Arg·X^-, where X = Cl, Br or I in the spectral region 850–1900 cm^{-1}. These amino acids constitute the extremes of gas-phase acidity and basicity values for the naturally occurring amino acids and therefore are expected to have a high propensity to form zwitterionic structures. Effects of anion size on the zwitterion stability of these amino acids are investigated using comparison to IRMPD spectra of corresponding metal cationized complexes and hybrid density functional theory to aid in spectral interpretation.

2. Experimental

2.1. IRMPD spectroscopy

All experiments were performed using a 4.7 T Fourier-transform ion cyclotron resonance mass spectrometer and a free electron laser (FELIX) which provides intense tunable infrared radiation in the mid-IR (850–1900 cm^{-1}). Descriptions of the instrument [49] and experimental parameters [31] are presented elsewhere. Ions were generated by electrospray ionization from 20/80 water/methanol solutions of Glu, His, or Arg and LiCl, $BaBr_2$, or NaI at 1–2 mM concentrations of the amino acid and halide salt. Solutions were infused at a rate of 10–20 μL/min. All chemicals were obtained from Sigma–Aldrich, Steinheim, Germany. Precursor complexes were isolated using stored waveform inverse Fourier transforms [50] and subsequently irradiated for 2.5–3.5 s using tunable radiation from FELIX with a macropulse rate of 5 Hz. A single irradiation time was used for each complex and was selected to produce extensive, but not complete, photodissociation at the peak intensity of each spectrum.

2.2. Computations

Candidate low-energy structures of Glu·Cl^-, His·Cl^-, and Arg·Cl^- were generated using Monte Carlo conformational searching and the MMFFs force field as implemented in *Macromodel 9.7* (Schrodinger, Inc. Portland, OR). At least 10,000 conformations were identified for each complex. Low-energy conformers were then grouped into families with similar structures and representative conformers from each family were selected for quantum mechanical geometry optimization in *Q-Chem v. 3.1* [51]. Structures with Br^- and I^- were generated by halide ion substitution into the chloridated structures. Geometries of the resulting structures were optimized at the B3LYP/6−31+G** level of theory using the CRENBL basis set and effective core potential for Br^- and I^- [52,53].

Vibrational frequencies and intensities were calculated using the double-harmonic approximation and the analytical Hessian of the energy-minimized structures using *Q-Chem v. 3.1*. Each of the resulting structures was found to have all real harmonic vibrational frequencies at this level of theory indicating that they are local minima on the potential energy surface. Zero-point energies and 298 K enthalpies and entropies were calculated using unscaled harmonic vibrational frequencies, and 298 K relative Gibbs free energies were obtained using these data. Calculated infrared absorption spectra are plotted with frequencies scaled by 0.975, a factor found to provide reasonable agreement between experimental spectra and calculated spectra at this level of theory in other IRMPD studies of amino acid complexes in this spectral region [19–21,29,30,37,39–41,54]. The intensities are convolved with a 40 cm^{-1} full width at half maximum (fwhm) Lorentzian profile to approximate the experimental peak shapes.

3. Results

3.1. Fragmentation

IRMPD of Glu·X^-, His·X^- and Arg·X^-, where X = Cl, Br, or I, results predominantly in the formation of X^- or loss of HX. For Arg·Cl^-, a minor product corresponding to the loss of (CN_2H_3 + Cl) was also observed, presumably resulting from subsequent dissociation of the primary product ion. Formation of Cl^- was not observed, whereas for the iodated amino acids, I^- was the primary (Glu) or only (His and Arg) product ion formed. Based on anion size, the binding energy of I^- should be less than that of Cl^-, so I^- should be more readily lost from the amino acids. In addition, HCl has a weaker gas-phase acidity (1372 kJ/mol) [55], compared to HI (1293.7 kJ/mol) [56], which should favor formation and loss of HCl. The IRMPD reaction pathways of each precursor are given in Table 1. By comparison, IRMPD of protonated and metal cationized Arg and Glu results in loss of water and other neutrals, and for cesiated complexes, loss of Cs^+ [30,32].

3.2. Spectroscopy

The IRMPD spectral intensity at a given frequency is calculated as a yield from the measured intensities of the precursor and product ions, I_{prec} and I_{prod}, respectively, corrected for the frequency dependent laser power $P(\omega)$.

$$\text{IRMPD spectral intensity (yield)} = (P(\omega))^{-1} \times \frac{\sum I_{prod}}{\sum I_{prod} + I_{prec}}$$

An IRMPD spectrum of each precursor ion is reported as the IRMPD spectral intensity as a function of laser frequency, normalized to the peak intensity of the most intense band. IRMPD spectra obtained using this photodissociation yield method are less directly comparable to linear absorption spectra than the laser-induced photodissociation rate constant method as discussed by Prell et al. [57]. However, this method provides spectra that are directly comparable to those reported previously for many cationized or deprotonated amino acids in this spectral region [17–23,25–34,36–41,54]. The IRMPD spectra of Glu·X^-, His·X^- and Arg·X^-, where X = Cl, Br, and I, from ~850 to 1900 cm^{-1} are shown in Fig. 1. Structural information from these spectra is obtained

Table 1
IRMPD products of anionized amino acid complexes.

Anion	Glutamic acid		Histidine	Arginine	
Cl^-	–HCl		–HCl	–HCl (85%)	$-(CN_2H_3+Cl)$ (15%)
Br^-	–HBr (75%)	Br^- (25%)	Br^-	N/A	N/A
I^-	–HI (20%)	I^- (80%)	I^-	I^-	

from comparisons to previously reported spectra of protonated and metal cationized amino acids and from comparisons to calculated spectra of candidate low-energy structures.

The IRMPD spectra of Glu·Cl^-, Glu·Br^-, and Glu·I^- are similar with common features centered at ~1750 and 1375 cm^{-1} in each spectrum. For Glu·I^- and Glu·Br^-, a weak band is observed at ~1600 cm^{-1}, and for Glu·I^- there are additional minor bands at ~1200 and 1040 cm^{-1}. The band at ~1750 cm^{-1} is narrower for Glu·Cl^- (~40 cm^{-1} fwhm) than for Glu·Br^- (~75 cm^{-1} fwhm), and this feature for Glu·I^- consists of two partially resolved peaks at 1755 and 1775 cm^{-1}. The centroid of this feature blueshifts with increasing anion size. These bands correspond to the carbonyl stretching modes of the two carboxylic acid groups of Glu [30], indicating that Glu is nonzwitterionic in these complexes (vide infra). The band at ~1375 cm^{-1} for Glu·Cl^- is relatively narrow and appears as a single band whereas for Glu·Br^-, this feature is composed of two poorly resolved bands at ~1370 and 1400 cm^{-1} and a shoulder from ~1275 to 1175 cm^{-1}. Bands contributing to this feature for Glu·I^- are not resolved. The weak band observed at ~1600 cm^{-1} for Glu·I^- and Glu·Br^- is consistent with an NH_2 scissoring bend, and the feature at ~1375 cm^{-1} for Glu·X^- is similar to that observed for Glu·M^+ and corresponds to hydrogen bonded NH and CH bends [30].

The IRMPD spectra for His·X^- complexes have many well resolved bands in the region between 850 and 1850 cm^{-1}. The spectra for His·Cl^- and His·Br^- are quite similar in that they both contain the same 10 bands (~1750, 1600, 1570, 1475, 1410, 1350, 1230, 1190, 1100, 1000 and 915 cm^{-1}) albeit with some small differences in the relative intensities of the bands. The spectrum of His·I^- includes all of these bands and an additional feature at ~1710 cm^{-1}. Similar to the Glu spectra, the carbonyl stretch near 1750 cm^{-1} blueshifts by ~10 cm^{-1} with increasing anion size from Cl^- to I^-. The carbonyl stretching bands at ~1750 cm^{-1} indicate that His is predominantly nonzwitterionic, as does the band at 1710 cm^{-1} which indicates some contribution from an additional structure with a different chemical environment for the carboxylic acid group [28].

The IRMPD spectra of Arg·Cl^- and Arg·I^- are very similar and each has a broad band (~125 cm^{-1} fwhm), centered at ~1625 cm^{-1} in addition to broad photodissociation below 1500 cm^{-1} with two poorly resolved features at ~1475 and 1350 cm^{-1} that have low signal-to-noise ratios. There is also a very weak band at ~1740 cm^{-1}. The band at ~1625 cm^{-1} corresponds to contributions from the antisymmetric carbonyl stretch of a carboxylate group and hydrogen bonded NH bending modes, consistent with a zwitterionic structure of Arg [32]. This band is close in frequency to the carboxylate stretch band observed at ~1630 cm^{-1} in the IRMPD spectra of deprotonated Trp, Phe, Tyr and Cys [48].

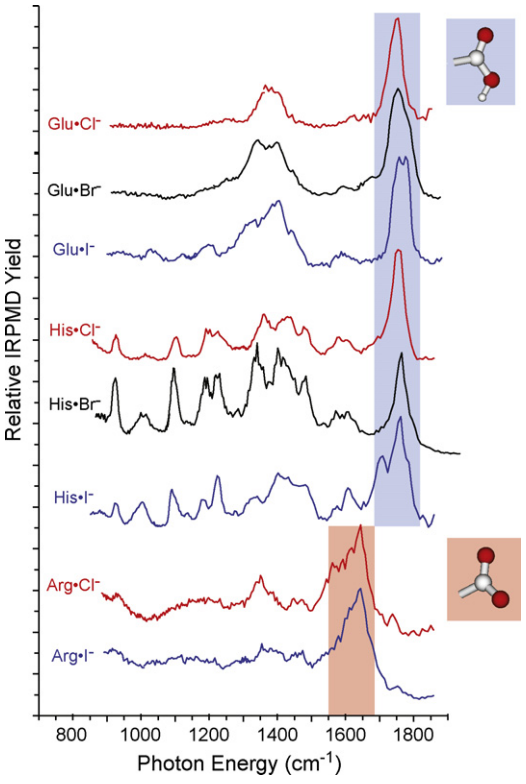

Fig. 1. IRMPD spectra of Glu·X^-, His·X^- and Arg·X^-, X = Cl^-, Br^-, or I^- at 298 K. Diagnostic carbonyl stretching bands indicating nonzwitterionic (1685–1825 cm^{-1}) or zwitterionic (1550–1685 cm^{-1}) forms of the amino acids in these complexes are indicated on the spectra.

3.3. Calculated structures

Representative structures of low-energy conformers for Glu·X^-, His·X^- and Arg·X^- are shown in Figs. 2–4, respectively, along with their calculated spectra and relative 0/298 K Gibbs free energies at the B3LYP/6−31+G**/CRENBL level of theory (Table 2). The calculated structures and spectra differ only slightly for the different halide anions. For example, the calculated spectrum of the lowest energy structure for Glu·Cl^- is nearly indistinguishable from those calculated for the same structure with Br^- and I^-, although there is a slight blueshift (~5–10 cm^{-1}) in the carbonyl stretches of the carboxylic acids with increasing anion size (Fig. 5), consistent with

Table 2
Relative Gibbs free energies (kJ/mol) of low-energy structures at 0/298 K calculated at the B3LYP/6−31+G**/CRENBL level of theory.

Structure	Cl^-	Br^-	I^-
Glu			
$GluNO_C$	7.0/6.2	0/0	0/0
$GluO_SO_C$	0/0	5.6/5.3	8.9/10.5
$GluNO_SO_C$	29.8/31.3	23.3/23.8	28.0/24.5
GluZW	22.8/20.0	19.0/18.2	18.3/19.0
His			
$HisN_\tau$	1.8/0	10.3/8.9	7.0/6.6
$HisN_\tau N_\pi$	0/2.1	0/0	0/0
HisZW	19.2/17.6	21.0/22.7	24.8/22.3
$HisN_\pi O$	6.9/8.5	6.3/5.5	12.8/17.3
$HisN_\tau N_\pi O$	9.8/11.3	10.2/13.4	14.1/18.3

Structure	Cl^-	I^-
Arg		
A	0.1/0	0.1/0
B	0/3.8	0/3.8
C	4.5/12.7	2.1/8.9
D	4.9/8.5	1.1/5.0

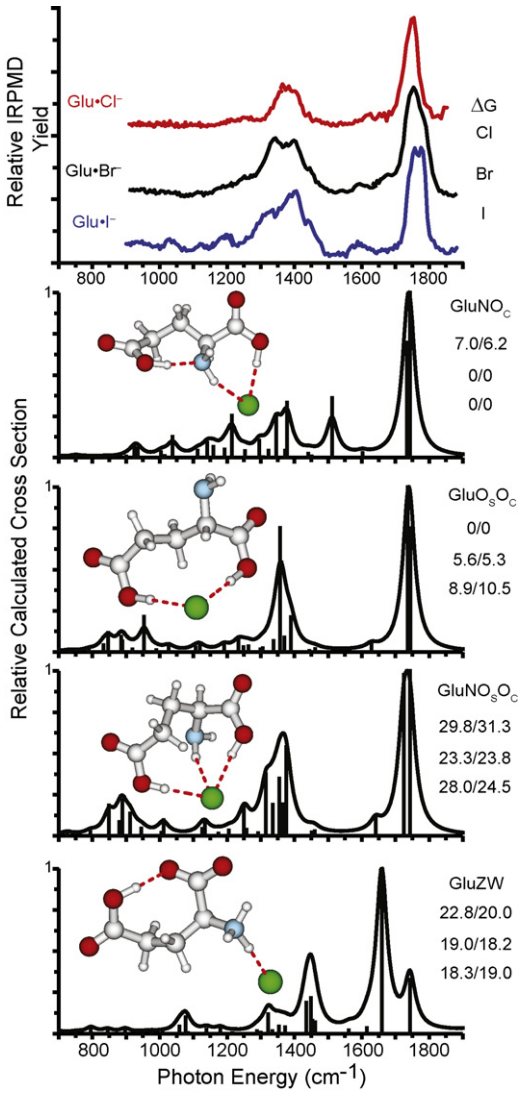

Fig. 2. Measured IRMPD spectra of Glu·X⁻, X = Cl⁻, Br⁻, or I⁻ (top), and calculated low-energy structures and spectra for Glu·Cl⁻. Relative Gibbs free energies in kJ/mol at 0/298 K calculated using the B3LYP/6–31+G**/CRENBL level of theory are indicated for each structure and anion.

the measured spectra for these complexes (Fig. 1). A corresponding increase in the OH bond length, indicative of increased carboxylate character, is calculated to occur with decreasing anion size for nonzwitterionic structures where the hydroxyl hydrogen atom interacts with the anion or a strongly basic site. The representative structures and spectra shown in Figs. 2–4 are those of the chloridated complexes, and the relative Gibbs free energies (kJ/mol) for all three anions at zero and 298 K are indicated for each structure.

3.3.1. *Glu·X⁻ structures*

Four structural families are identified from conformational searching of Glu·Cl⁻: a nonzwitterionic structure, GluNO$_C$, in which the anion interacts with the N-terminus and the OH group of the C-terminus (O$_C$), and the carboxylic acid group of the side chain donates a hydrogen bond to the N-terminus; GluO$_S$O$_C$ where both the side chain (O$_S$) and C-terminal OH groups coordinate to the anion; GluNO$_S$O$_C$, in which the N-terminus, side chain, and C-terminal OH groups all coordinate to the anion; and GluZW, where the protonated N-terminus of zwitterionic Glu coordinates to the anion, and a hydrogen is shared between C-terminal and side chain carbonyl oxygen atoms. The lowest energy structures are GluNO$_C$ for Br⁻ and I⁻ and GluO$_S$O$_C$ for Cl⁻. Structures GluNO$_S$O$_C$ and GluZW are substantially higher in energy by ~30 and 20 kJ/mol, respectively.

3.3.2. *His·X⁻ structures*

Six structural families are identified from conformational searching of His·Cl⁻: five low-energy nonzwitterionic structures and the lowest energy zwitterionic structure are shown in Fig. 3. The side chain of His has two nitrogen atoms, designated 'pros' (near) and 'tele' (far) to indicate their distance from the tertiary carbon of the imidazole group, and they are abbreviated N$_\pi$ and N$_\tau$ respectively. Each of these nitrogen atoms may bind a hydrogen atom, although not both at the same time without forming a zwitterionic structure. The nonzwitterionic structures are characterized by different coordinations of the anion. For the HisN$_\tau$ structure, the anion binds only to the tele-NH group and the pros-nitrogen atom accepts a hydrogen bond from the N-terminus (N$_T$). This is the lowest energy structure at 298 K for His·Cl⁻. The lowest energy structure for His·Br⁻ and His·I⁻ is HisN$_T$N$_\pi$ where the pros-NH and the N-terminus coordinate to the anion and the C-terminus donates a weak hydrogen bond to the N-terminus. HisN$_\pi$O and HisN$_T$N$_\pi$O both have coordination of the C-terminus to the anion along with one or two of the NH groups, respectively. For HisZW, the protonated N-terminus of His coordinates to the anion and the pros-NH donates a hydrogen bond to an oxygen atom of the carboxylate group.

3.3.3. *Arg·X⁻ structures*

Four structural families are identified from conformational searching for Arg·Cl⁻: three zwitterionic structures and the lowest energy nonzwitterionic structure are shown in Fig. 4. The un-protonated side chain nitrogen atoms are designated ε, η, and η′, as indicated in Fig. 4, where ε is the secondary amine nitrogen atom, η is the primary imine nitrogen atom, and η′ is the primary amine nitrogen atom. For zwitterionic structures where the side chain is protonated, we retain the η and η′ labels inherited from the un-protonated structures for convenience. For structure ArgZW-A, the ε-NH donates a hydrogen bond to the deprotonated C-terminus and the anion coordinates to the other two NH groups of the protonated side chain. In structure ArgZW-B, the η-NH group of the protonated side chain donates a hydrogen bond to the deprotonated C-terminus, and both the ε- and η′-NH groups coordinate to the anion. These two structures are very similar and nearly isoenergetic. Structure ArgZW-C differs somewhat in that the deprotonated C-terminus accepts two hydrogen bonds, one each from the ε- and η′-NH groups of the protonated side chain, and the anion is coordinated by both the η′- and η-NH groups. Structure ArgNZ-D is nonzwitterionic and is analogous to structure ArgZW-B with a proton transferred from the η-nitrogen to the C-terminus.

4. Discussion

4.1. *Comparison with cationized spectra*

Cs⁺ and Cl⁻ have nearly the same ionic radii (167 pm) [58], and the carbonyl band in the spectra of Glu·Cs⁺ and Glu·Cl⁻ is remarkably similar in both frequency (1760 and 1755 cm^{-1}, respectively) and peak shape [30]. Similarly, the antisymmetric carbonyl stretch bands of the carboxylate group for Arg·Cs⁺ and Arg·Cl⁻ are close in frequency, centered at ~1615 and 1625 cm^{-1}, respectively [32]. The similarity of the carbonyl bands in the spectra of cesiated and chloridated Glu and Arg indicates that the sign of the ion's charge plays little role in these vibrational frequencies, although the binding sites of metal cations versus halide anions in these complexes are different. The metal cation in Glu·M⁺ and His·M⁺ for nonzwitterionic structures attaches to one or more carbonyl oxygen atoms and

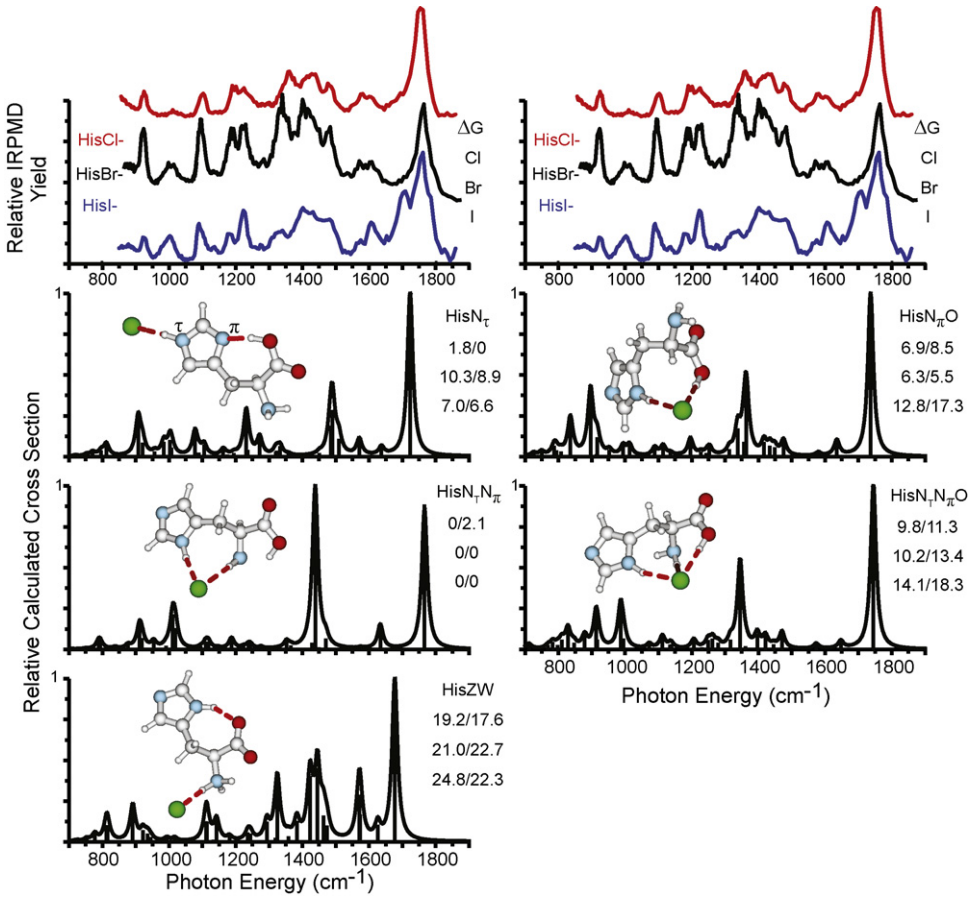

Fig. 3. Measured IRMPD spectra of His·X$^-$, X = Cl$^-$, Br$^-$, or I$^-$ (top), and calculated low-energy structures and spectra for His·Cl$^-$. Relative Gibbs free energies in kJ/mol at 0/298 K calculated using the B3LYP/6–31+G**/CRENBL level of theory are indicated for each structure and anion.

corresponding free-OH bends are observed at ~1150–1170 cm^{-1}. For Glu·X$^-$ and His·X$^-$, no hydroxyl bends are evident in the experimental spectra indicating that the OH groups are coordinated to the anion or are hydrogen bonded.

For His·X$^-$, the bands below 1700 cm^{-1} are especially intriguing because they are not apparent in the IRMPD spectrum of His·Na$^+$, the only IRPD spectrum reported for alkali metal cationized His [28]. The most intense band in the spectrum of His·Na$^+$ occurs at ~1150 cm^{-1} and corresponds to the free-OH bend of the carboxylic acid group. An intense band corresponding to the same mode at ~1150 cm^{-1} also occurs for HisArg·H$^+$ [40]. Its absence in the anionized spectra is consistent with the OH group donating a hydrogen bond or coordinating to the anion. The bands below 1700 cm^{-1} are unusually sharp and likely correspond to vibrations associated with the rigid imidazole ring.

The band at 1625 cm^{-1} for Arg·X$^-$ and the absence of any intense bands above 1700 cm^{-1} are consistent with predominantly zwitterionic structures of Arg, as observed for Arg·M$^+$, where M = K, Rb, and Cs [32]. The broad dissociation and poorly resolved bands below 1500 cm^{-1} in the Arg·X$^-$ spectra prohibit further structural conclusions from the experimental spectra. However, broad dissociation with poorly resolved spectral features has been observed for other amino acid complexes containing strong intramolecular hydrogen bonds [26,48]. The assignment of zwitterionic structures for both Arg·X$^-$ and Arg with an excess electron attached [45,46] indicates that the stabilization of the large dipole of the zwitterionic form by the anion in these zwitterionic structures outcompetes solvation of the anion by hydrogen bonding in nonzwitterionic structures. Evidently, solvation of the charge by hydrogen bonds in these complexes is less effective than the charge solvation by heteroatoms observed for the nonzwitterionic forms of Arg·Li$^+$ and Arg·Na$^+$ [32] and is likely attributable to the relatively large size of the anions.

The IRMPD spectra for each anionized amino acid are very similar indicating that anion size has little effect on the conformations adopted for each of these complexes. Only the spectrum for His·I$^-$ indicates a clear structural change as a function of ion size. In contrast, effects of ion size on structure have been reported for many metal cationized amino acid complexes, including Glu·M$^+$ [30], Arg·M$^+$ [24,32], Lys·M$^+$ [19], and Met·M$^+$ [25]. For example, the differences observed between the IRMPD spectra of Arg·Li$^+$ and Arg·Na$^+$ indicate a switch from a nonzwitterionic structure of Arg when bound to Li to primarily zwitterionic Arg when bound to Na$^+$ [24,32].

4.2. Origins of carbonyl stretch redshifting

The carbonyl band in the IRMPD spectra of both Glu·Cs$^+$ (1760 cm^{-1}) and Glu·Cl$^-$ (1755 cm^{-1}) is redshifted relative to that of a free carboxylic acid (~1780 cm^{-1} for gas-phase acetic acid) [59]. The carboxylate antisymmetric stretch for Arg·Cs$^+$(1615 cm^{-1}) and Arg·Cl$^-$ (1625 cm^{-1}) [32] is similar to that of benzoate at ~1630 cm^{-1} [60], which is likely redshifted from that of a free carboxylate due to electron donation from the benzene ring. Further redshifting of carbonyl bands with increasing charge state has also been reported for alkali metal and alkaline earth metal cationized amino acids and peptides, including Glu [30], His [28], and Asn [29]. This increasing carbonyl stretch redshift as a function of charge state for metal cationized amino acids and peptides has been attributed to transfer of electron density from the carbonyl to

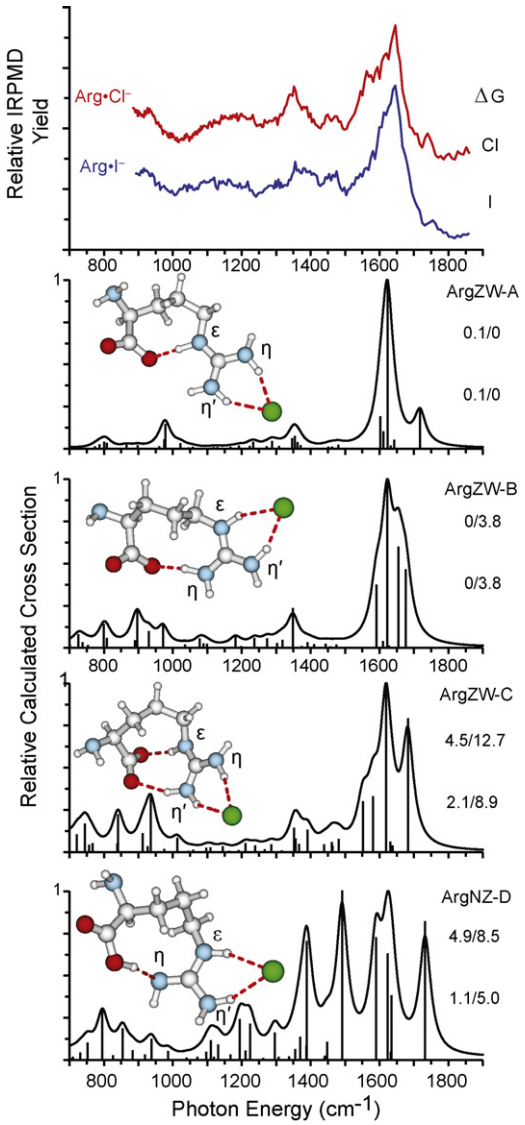

Fig. 4. Measured IRMPD spectra of Arg·X⁻, X = Cl⁻, or I⁻ (top), and calculated low-energy structures and spectra for Arg·Cl⁻. Relative Gibbs free energies in kJ/mol at 0/298 K calculated using the B3LYP/6−31+G**/CRENBL level of theory are indicated for each structure and anion.

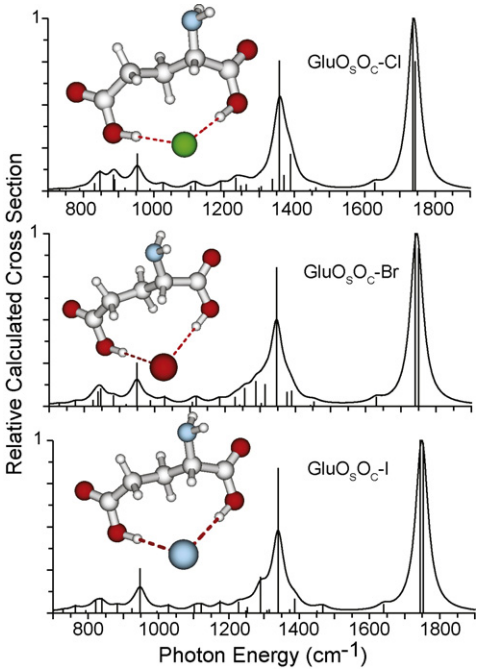

Fig. 5. $GluO_SO_C$ structures and spectra for Glu complexed with Cl⁻, Br⁻, and I⁻ calculated using the B3LYP/6−31+G**/CRENBL level of theory.

the attached metal ion which increases with increasing metal ion charge state [30,41].

In the absence of other effects, an attached halide ion would be expected to transfer electron density to the amino acid resulting in a *blueshift* of the carbonyl stretch band, thus the observed carbonyl stretch redshift for the complexes investigated cannot be fully explained by this charge transfer effect. Instead, this carbonyl stretch redshift for both anionized and cationized amino acids and peptides can be primarily attributed to two other factors: the favorable alignment of the dipole moment of the carbonyl with the ion's electric field, and for halidated complexes, partial proton transfer from the carboxylic acid to the halide anion which results in partial carboxylate character. Because cations attach to the complexes close to the carbonyl oxygen whereas anions attach closer to the carbonyl carbon for nonzwitterionic structures, the interaction of the carbonyl dipole moment with the ion's electric field is favorable for ions of either polarity, causing a redshift in the carbonyl stretch frequency, i.e., a Stark effect.

The carbonyl band redshifts for Glu·X⁻ and His·X⁻ with decreasing halide ion size by ~10 cm^{-1} from X = I to X = Cl, and this effect provides additional evidence that the redshift is caused by the electric field of the ion. By comparison, the carbonyl stretch band in the spectrum of $GluLi^+$ is redshifted from the corresponding band for $Glu{\cdot}Cs^+$ by ~20 cm^{-1}. A similar shift has been observed between the lithiated and cesiated spectra of other amino acids, including Gln [20], Trp [33], Ser [23], and Thr [34]. The anion size-dependent shift observed for Glu·X⁻ and His·X⁻ is likely smaller than for $Glu{\cdot}M^+$ because the halide ions are much larger (Cl^-, Br^- and I^-: 167, 196 and 220 pm) than the alkali metal cations (Li^+ and Cs^+: 76 and 167 pm) [58] and are further away from the carbonyl groups, resulting in a more subtle change in the ion's electrostatic potential as experienced by the carbonyl group. For both anionized and cationized zwitterionic Arg, any change in the frequency of the carboxylate antisymmetric shift with decreasing ion size appears to be obfuscated by contributions from hydrogen bonded NH bending modes that occur in the same region.

The redshift in the carbonyl stretch from that of a neutral carboxylic acid group is in fact slightly *greater* for $Glu{\cdot}Cl^-$ than for $Glu{\cdot}Cs^+$, despite the latter having a much shorter carbonyl-ion distance. Thus, other factors, in addition to the Stark shift, must contribute. Chloride anion is substantially less acidic in the gas phase than are Br^- and I^-, which causes the strength of the interaction between the halide ion and adjacent carboxylic acid hydrogen atom(s) to increase with decreasing halide ion size. This results in increased partial carboxylate character of the carboxylic acid group with decreasing ion size, consistent with the surprisingly large redshifting effects of the halide ions described above. This sharing of the hydrogen atom between the hydroxyl oxygen atom and halide anion is analogous to the sharing of a proton between heteroatoms observed in proton-bound dimeric complexes, where spectral frequencies can be highly sensitive to the difference in proton affinity of the substituents [61].

4.3. Comparisons with theory

The calculated spectra of the lowest energy structures are generally consistent with the experimental spectra, although there is evidence for multiple structures for some of these complexes. The

carbonyl band in the calculated spectra blueshifts by ~5–10 cm^{-1} with increasing ion size from Cl^- to I^-. For example, the carbonyl band in structure $GluO_SO_C$ occurs at ~1740, 1745 and 1750 cm^{-1} for Cl^-, Br^- and I^-, respectively (Fig. 5). A corresponding decrease in the hydroxyl OH bond distance with increasing ion size, and hence, decreasing carboxylate character, is calculated for this structure. Similar shifts are observed in the calculated spectra for the other nonzwitterionic structures and are consistent with the experimental spectra of Glu·X^-, which show a ~10 cm^{-1} blueshift for this band for these same anions. For the zwitterionic structure, GluZW, the carboxylate band is the same for Cl^- and Br^-, but blueshifts by ~5 cm^{-1} for I^-. Contributions to the experimental spectra from specific low-energy structures are discussed in detail below.

4.3.1. Glu·X^-, X = Cl, Br, and I

The carbonyl stretches of the carboxylic acid groups in Glu·Cl^- have similar frequencies resulting in a single band at ~1740 cm^{-1} in the calculated spectra of the nonzwitterionic structures, in agreement with the experimental spectra (Fig. 2). The calculated spectra of the zwitterionic structures differ substantially with two carbonyl bands at ~1660 and 1740 cm^{-1} corresponding to carbonyl stretches of the deprotonated C-terminus and the side chain carboxylic acid, respectively. These calculated spectra support assignment of the experimental spectra to one or more nonzwitterionic structures. The calculated spectrum of $GluO_SO_C$ provides good agreement with the experimental spectrum of Glu·Cl^-. The intense mode predicted at ~1350 cm^{-1} corresponds to the coupled, in-phase OH bending modes of the two carboxylic acid groups coordinating to the anion and likely contributes to the band observed in the experimental spectra at ~1375 cm^{-1} for all three anions. The calculated spectrum of $GluNO_C$ differs from that of $GluO_SO_C$ only slightly with a band predicted at ~1500 cm^{-1} corresponding to the bonded OH bending mode of the side chain carboxylic acid group hydrogen bonded to the N-terminus. This band is not evident in any of the experimental spectra. However, differences in relative intensities between IRMPD and calculated absorption spectra, especially for structures with strong hydrogen bonds, can be attributed to a number of factors, including uncertainties in the calculated intensities and other factors discussed elsewhere [41]. The calculated spectrum of $GluNO_SO_C$ is very similar to that of $GluO_SO_C$, with some differences in the bonded NH/OH bending feature at ~1350 cm^{-1}. This structure is calculated to be much higher in energy, but contributions from such structures cannot be eliminated based on comparison to the experimental data alone.

4.3.2. His·X^-, X = Cl, Br, and I

No calculated spectrum of a single conformer can account for all of the bands observed in the experimental spectra of His·X^- (Fig. 3). However, the band at ~1750 cm^{-1} in the IRMPD spectrum of His·X^- is most consistent with a substantial contribution to the ion population from structures like $HisN_TN_\pi$, where the frequency of the carbonyl stretching mode is significantly blueshifted relative to the carbonyl bands of the other nonzwitterionic structures. The frequency of the carbonyl stretch for the zwitterionic structure HisZW is ~1680 cm^{-1}, supporting assignment of the experimental spectra to nonzwitterionic structures. For His·I^-, the band at ~1710 cm^{-1} can be attributed to contributions from the other nonzwitterionic structures. For $HisN_T$, the hydrogen bond between the C-terminus and the pros-nitrogen atom should be strong due to the excellent alignment and high basicity of the side chain, and the strongly shared hydrogen atom likely gives the carbonyl partial carboxylate character, redshifting the carbonyl stretch. The redshifted carbonyl band at 1710 cm^{-1} is not observed for the other anions indicating minimal contribution from this type of structure in the other complexes. The lower frequency bands are more challenging to assign, but could be more readily identified by measuring IRMPD spectra of His derivatives or by isotopic substitution. The IR spectrum of condensed-phase imidazole, an analogue for the histidine side chain, has many bands between 800 and 1700 cm^{-1} corresponding to CN stretches, ring stretching modes, and NH and CH bends [62]. However, the frequencies of these modes do not consistently match those observed in the IRMPD spectra of His·X^-, complicating assignment based on these data.

4.3.3. Arg·X^-, X = Cl, and I

The calculated spectra of structures ArgZW-A and ArgZW-B provide reasonable agreement with the broad experimental band at ~1625 cm^{-1} (Fig. 4). These results are consistent with assignment of Arg·X^- to predominantly zwitterionic structures. The weak band at ~1740 cm^{-1} may be due to the hydrogen bonded NH bend of the ε nitrogen in ArgZW-A (calculated at ~1720 cm^{-1}), but this band could also be due to a small population of nonzwitterionic structures, such as ArgNZ-D. Structure ArgZW-C also has a hydrogen bonded NH bend at ~1690 cm^{-1} that is not observed in the experimental spectra indicating that structure ArgZW-C is not the dominant structure. Bands attributed to this mode have been reported in the IRMPD spectra of alkali metal cationized Arg indicating a difference between the zwitterionic structures adopted for the anionized and cationized complexes. The calculated spectra for structures ArgZW-A and ArgZW-B are very similar. Based on the calculations that indicate that these structures are nearly isoenergetic, it is likely that both are present in the ion population.

5. Conclusions

The IRMPD spectra of Glu·X^-, His·X^-, and Arg·X^-, where X = Cl, Br, or I, clearly show whether or not the amino acid adopts a zwitterionic form in these complexes. The spectra of Glu·X^- and His·X^- each have a strong band at ~1750 cm^{-1} corresponding to the carbonyl stretch of a carboxylic acid indicating that the nonzwitterionic form of the amino acid is dominant. An additional band at ~1710 cm^{-1} for His·I^- indicates that another structure with a redshifted carbonyl stretch is also present. The broad band at ~1625 cm^{-1} for Arg·X^-, corresponding to the antisymmetric stretch of a carboxylate group, clearly shows that Arg is zwitterionic in these complexes.

The frequencies of the carbonyl bands are similar for these amino acids with either Cl^- or Cs^+ attached. Thus, the sign of the ion's charge for these similarly sized ions has little effect on the frequency of these diagnostic bands. The coordination of cations to these amino acids is different from that of anions, resulting in a favorable alignment of the dipole moment of the carbonyl stretch with the electric field of ions of either polarity, which causes a redshift in this band, i.e., a Stark effect. The slight redshift (~10 cm^{-1}) of the carbonyl band at ~1750 cm^{-1} for Glu·X^- and His·X^- with decreasing anion size is consistent with both a Stark effect and a more subtle effect of greater carboxylate character when smaller halide ions coordinate to the carboxylic acid group. The calculated spectra of the lowest energy structures generally provide good agreement with the experimental spectra. The IRMPD spectra of His·X^- have many sharp bands due to the side chain that do not correspond closely enough in frequency to features observed in the FT-IR spectrum of condensed-phase imidazole or in calculated spectra of low-energy conformers of His·X^- to make unambiguous assignments. Additional structural information could be obtained by measuring IRMPD spectra of analogous compounds or by isotopic labeling.

Acknowledgements

IRMPD spectra were measured at the FOM Institute for Plasma Physics "Rijnhuizen", which is financially supported by the Nederlandse Organisatie voor Wetenschappelijk Onderzoek (NWO). The authors thank Dr. Britta Redlich and the rest of the FELIX staff for excellent support. Generous financial support was provided by the National Science Foundation (Grants CHE-0718790 and OISE-730072).

References

[1] J.A. Loo, Mass Spectrom. Rev. 16 (1997) 1–23.
[2] E. Pidcock, G.R. Moore, J. Biol. Inorg. Chem. 6 (2001) 479–489.
[3] A.M. Pyle, J. Biol. Inorg. Chem. 7 (2002) 679–690.
[4] S. Frings, D. Reuter, S.J. Kleene, Prog. Neurobiol. 60 (2000) 247–289.
[5] U. Misgeld, R.A. Deisz, H.U. Dodt, H.D. Lux, Science 232 (1986) 1413–1415.
[6] A.N. Mayeno, A.J. Curran, R.L. Roberts, C.S. Foote, J. Biol. Chem. 264 (1989) 5660–5668.
[7] M. Chesler, Physiol. Rev. 83 (2003) 1183–1221.
[8] J.M. Russell, W.F. Boron, Nature 264 (1976) 73–74.
[9] J.R. Riordan, J.M. Rommens, B.S. Kerem, N. Alon, R. Rozmahel, Z. Grzelczak, J. Zielenski, S. Lok, N. Plavsic, J.L. Chou, M.L. Drumm, M.C. Iannuzzi, F.S. Collins, L.C. Tsui, Science 245 (1989) 1066–1072.
[10] F. Hofmeister, Arch. Exp. Pathol. Pharmacol. 24 (1888) 247–260.
[11] W. Kunz, J. Henle, B.W. Ninham, Curr. Opin. Colloid Interface Sci. 9 (2004) 19–37.
[12] X. Chen, T. Yang, S. Kataoka, P.S. Cremer, J. Am. Chem. Soc. 129 (2007) 12272–12279.
[13] M.G. Freire, C.M.S.S. Neves, A.M.S. Silva, L.M.N.B.F. Santos, I.M. Marrucho, L.P.N. Rebelo, J.K. Shah, E.J. Maginn, J.A.P. Coutinho, J. Phys. Chem. B 114 (2010) 2004–2014.
[14] L.M. Pegram, M.T. Record, J. Phys. Chem. B 111 (2007) 5411–5417.
[15] J.D. Smith, R.J. Saykally, P.L. Geissler, J. Am. Chem. Soc. 129 (2007) 13847–13856.
[16] J.S. Uejio, C.P. Schwartz, A.M. Duffin, W.S. Drisdell, R.C. Cohen, R.J. Saykally, Proc. Natl. Acad. Sci. U.S.A. 105 (2008) 6809–6812.
[17] M.F. Bush, J. Oomens, R.J. Saykally, E.R. Williams, J. Am. Chem. Soc. 130 (2008) 6463–6471.
[18] R.C. Dunbar, N.C. Polfer, J. Oomens, J. Am. Chem. Soc. 129 (2007) 14562–14563.
[19] M.F. Bush, M.W. Forbes, R.A. Jockusch, J. Oomens, N.C. Polfer, R.J. Saykally, E.R. Williams, J. Phys. Chem. A 111 (2007) 7753–7760.
[20] M.F. Bush, J. Oomens, R.J. Saykally, E.R. Williams, J. Phys. Chem. A 112 (2008) 8578–8584.
[21] M.F. Bush, J. Oomens, E.R. Williams, J. Phys. Chem. A 113 (2009) 431–438.
[22] P.B. Armentrout, E.I. Armentrout, A.A. Clark, T.E. Cooper, E.M.S. Stennett, D.R. Carl, J. Phys. Chem. B 114 (2010) 3927–3937.
[23] P.B. Armentrout, M.T. Rodgers, J. Oomens, J.D. Steill, J. Phys. Chem. A 112 (2008) 2248–2257.
[24] M.F. Bush, J.T. O'Brien, J.S. Prell, R.J. Saykally, E.R. Williams, J. Am. Chem. Soc. 129 (2007) 1612–1622.
[25] D.R. Carl, T.E. Cooper, J. Oomens, J.D. Steill, P.B. Armentrout, Phys. Chem. Chem. Phys. 12 (2010) 3384–3398.
[26] M.K. Drayss, D. Blunk, J. Oomens, B. Gao, T. Wyttenbach, M.T. Bowers, M. Schäfer, J. Phys. Chem. A 113 (2009) 9543–9550.
[27] M.K. Drayss, D. Blunk, J. Oomens, M. Schäfer, J. Phys. Chem. A 112 (2008) 11972–11974.
[28] R.C. Dunbar, A.C. Hopkinson, J. Oomens, C.K. Siu, K.W.M. Siu, J.D. Steill, U.H. Verkerk, J.F. Zhao, J. Phys. Chem. B 113 (2009) 10403–10408.
[29] A.L. Heaton, V.N. Bowman, J. Oomens, J.D. Steill, P.B. Armentrout, J. Phys. Chem. A 113 (2009) 5519–5530.
[30] J.T. O'Brien, J.S. Prell, J.D. Steill, J. Oomens, E.R. Williams, J. Phys. Chem. A 112 (2008) 10823–10830.
[31] N.C. Polfer, J. Oomens, D.T. Moore, G. von Helden, G. Meijer, R.C. Dunbar, J. Am. Chem. Soc. 128 (2006) 517–525.
[32] M.W. Forbes, M.F. Bush, N.C. Polfer, J. Oomens, R.C. Dunbar, E.R. Williams, R.A. Jockusch, J. Phys. Chem. A 111 (2007) 11759–11770.
[33] N.C. Polfer, J. Oomens, R.C. Dunbar, Phys. Chem. Chem. Phys. 8 (2006) 2744–2751.
[34] M.T. Rodgers, P.B. Armentrout, J. Oomens, J.D. Steill, J. Phys. Chem. A 112 (2008) 2258–2267.
[35] A. Kamariotis, O.V. Boyarkin, S.R. Mercier, R.D. Beck, M.F. Bush, E.R. Williams, T.R. Rizzo, J. Am. Chem. Soc. 128 (2006) 905–916.
[36] C. Kapota, J. Lemaire, P. Maitre, G. Ohanessian, J. Am. Chem. Soc. 126 (2004) 1836–1842.
[37] N.C. Polfer, J. Oomens, R.C. Dunbar, ChemPhysChem 9 (2008) 579–589.
[38] N.C. Polfer, B. Paizs, L.C. Snoek, I. Compagnon, S. Suhai, G. Meijer, G. von Helden, J. Oomens, J. Am. Chem. Soc. 127 (2005) 8571–8579.
[39] J.S. Prell, T.G. Flick, J. Oomens, G. Berden, E.R. Williams, J. Phys. Chem. A 114 (2010) 854–860.
[40] J.S. Prell, J.T. O'Brien, J.D. Steill, J. Oomens, E.R. Williams, J. Am. Chem. Soc. 131 (2009) 11442–11449.
[41] J.S. Prell, M. Demireva, J. Oomens, E.R. Williams, J. Am. Chem. Soc. 131 (2009) 1232–1242.
[42] T. Wyttenbach, M. Witt, M.T. Bowers, J. Am. Chem. Soc. 122 (2000) 3458–3464.
[43] R.R. Julian, M.F. Jarrold, J. Phys. Chem. A 108 (2004) 10861–10864.
[44] A.S. Lemoff, M.F. Bush, E.R. Williams, J. Am. Chem. Soc. 125 (2003) 13576–13584.
[45] P. Skurski, J. Rak, J. Simons, M. Gutowski, J. Am. Chem. Soc. 123 (2001) 11073–11074.
[46] S.J. Xu, W.J. Zheng, D. Radisic, K.H. Bowen, J. Chem. Phys. 122 (2005) 091103.
[47] S.R. Kass, J. Am. Chem. Soc. 127 (2005) 13098–13099.
[48] J. Oomens, J.D. Steill, B. Redlich, J. Am. Chem. Soc. 131 (2009) 4310–4319.
[49] J.J. Valle, J.R. Eyler, J. Oomens, D.T. Moore, A.F.G. van der Meer, G. von Helden, G. Meijer, C.L. Hendrickson, A.G. Marshall, G.T. Blakney, Rev. Sci. Instrum. 76 (2005) 023103.
[50] A.G. Marshall, T.C.L. Wang, T.L. Ricca, J. Am. Chem. Soc. 107 (1985) 7893–7897.
[51] Y. Shao, L.F. Molnar, Y. Jung, J. Kussmann, C. Ochsenfeld, S.T. Brown, A.T.B. Gilbert, L.V. Slipchenko, S.V. Levchenko, D.P. O'Neill, R.A. DiStasio, R.C. Lochan, T. Wang, G.J.O. Beran, N.A. Besley, J.M. Herbert, C.Y. Lin, T. Van Voorhis, S.H. Chien, A. Sodt, R.P. Steele, V.A. Rassolov, P.E. Maslen, P.P. Korambath, R.D. Adamson, B. Austin, J. Baker, E.F.C. Byrd, H. Dachsel, R.J. Doerksen, A. Dreuw, B.D. Dunietz, A.D. Dutoi, T.R. Furlani, S.R. Gwaltney, A. Heyden, S. Hirata, C.P. Hsu, G. Kedziora, R.Z. Khalliulin, P. Klunzinger, A.M. Lee, M.S. Lee, W. Liang, I. Lotan, N. Nair, B. Peters, E.I. Proynov, P.A. Pieniazek, Y.M. Rhee, J. Ritchie, E. Rosta, C.D. Sherrill, A.C. Simmonett, J.E. Subotnik, H.L. Woodcock, W. Zhang, A.T. Bell, A.K. Chakraborty, D.M. Chipman, F.J. Keil, A. Warshel, W.J. Hehre, H.F. Schaefer, J. Kong, A.I. Krylov, P.M.W. Gill, M. Head-Gordon, Phys. Chem. Chem. Phys. 8 (2006) 3172–3191.
[52] M.M. Hurley, L.F. Pacios, P.A. Christiansen, R.B. Ross, W.C. Ermler, J. Chem. Phys. 84 (1986) 6840–6853.
[53] L.A. Lajohn, P.A. Christiansen, R.B. Ross, T. Atashroo, W.C. Ermler, J. Chem. Phys. 87 (1987) 2812–2824.
[54] R.C. Dunbar, J.D. Steill, N.C. Polfer, J. Oomens, J. Phys. Chem. B 113 (2009) 10552–10554.
[55] J.D.D. Martin, J.W. Hepburn, J. Chem. Phys. 109 (1998) 8139–8142.
[56] D. Hanstorp, M. Gustafsson, J. Phys. B: At. Mol. Opt. Phys. 25 (1992) 1773–1783.
[57] J.S. Prell, J.T. O'Brien, E.R. Williams, J. Am. Soc. Mass Spectrom. 21 (2010) 800–809.
[58] R.D. Shannon, Acta Crystallogr. A 32 (1976) 751–767.
[59] Coblentz Society, Inc., Evaluated infrared reference spectra, in: P.J. Linstrom, W.G. Mallard (Eds.), NIST Chemistry WebBook, NIST Standard Reference Database Number 69, National Institute of Standards and Technology, Gaithersburg, MD, p. 20899, http://webbook.nist.gov (retrieved 05.05.10).
[60] J. Oomens, J.D. Steill, J. Phys. Chem. A 112 (2008) 3281–3283.
[61] J.R. Roscioli, L.R. McCunn, M.A. Johnson, Science 316 (2007) 249–254.
[62] d.N.D. Marcia Cordes, J.L. Walter, Spectrochim. Acta A 24 (1968) 237–252.